Chinese Chemical Letters 35 (2024) 110022

Contents lists available at ScienceDirect

Chinese Chemical Letters

journal homepage: www.elsevier.com/locate/cclet

A cucurbit[8]uril-based supramolecular phosphorescent assembly: Cell imaging and sensing of amino acids in aqueous solution

Qian Ren, Xue Dai, Ran Cen, Yang Luo, Mingyang Li, Ziyun Zhang, Qinghong Bai, Zhu Tao, Xin Xiao*

Key Laboratory of Macrocyclic and Supramolecular Chemistry of Guizhou Province, Institute of Applied Chemistry, Guizhou University, Guiyang 550025, China

ARTICLE INFO

Article history:
Received 9 February 2024
Revised 1 May 2024
Accepted 16 May 2024
Available online 17 May 2024

Keywords:
Cucurbituril
Isobromoquinoline
Pure organic room-temperature phosphorescent
Cell imaging
Amino acid

ABSTRACT

In recent years, host-guest interactions of macrocycles have emerged as a promising approach to effectively enhance pure organic room-temperature phosphorescence by inhibiting the nonradiative relaxation while isolating the effects of oxygen and water molecules. In this work, a supramolecular assembly Q[8]-BCPI was constructed by 6-bromoisoquinoline derivative (BCPI) and cucurbit[8]uril (Q[8]). The assembly produced intense green room temperature phosphorescence (RTP) emission and enabled supramolecular recognition and detection of L-tryptophan (L-Trp) and L-tyrosine (L-Tyr). Moreover, the Q[8]-BCPI assembly showed good biocompatibility and low biotoxicity, and had a good staining effect on HeLa cells.

Room-temperature phosphorescent (RTP) materials are known for their large stokes shifts and extended lifetimes, making them more advantageous for bioimaging compared to fluorescent materials [1,2]. However, while these RTP materials are stable in the solid state, they tend to be unstable in a solution. Factors, such as dissolved oxygen and water in the solution, can lead to a nonradiative decay of the triplet excited state, thereby restricting the stability and applications of the RTP materials in aqueous solutions. This enhancement has been realized by various methods, including supramolecular host-guest interactions [3], polymers [4–6], heavy atom effects [7,8], *etc.* Notably, supramolecular host-guest interactions have provided a simple, yet effective, approach to obtain RTP emission in aqueous solutions. Macrocyclic host compounds, such as cyclodextrins [9,10], crown ethers [11–13], pillar[*n*]arenes [14], and cucurbit[*n*]urils (Q[*n*]s) [15–17], have been used to construct the RTP materials.

The Q[*n*]s have a rigid cavity that is hydrophobic inside and hydrophilic outside [18–31]. This special structure provides a favorable environment for the formation of RTP emission [32,33]. The Q[*n*]s encapsulate the guest molecules by non-covalent interactions, thereby restricting the disordered motion of these molecules and shielding them from the effects of quenchers in aqueous solutions [34,35]. There are many studies on the generation of RTP emission by the cavity-limited domains of the Q[*n*]s [36–38]. Recently, Liu *et al.* [39] used Q[8] and the 1,2-diaminocyclohexane-bridged 4-(4-bromophenyl)pyridinium salt to form a 1:1 supramolecular phosphorescent fold. They also used phosphorescence for the detection of antibiotics in water. Furthermore, Yang *et al.* [40] reported on a co-constructed rotaxane, which consisted of Q[6] and cyclodextrins, for the detection of amino acids. Also, Liu *et al.* reported on a series of works utilizing Q[*n*]s to generate room-temperature phosphorescence [3,41–43]. They then used the classical phosphorescent 6-bromoisoquinoline derivatives and 4-phenylpyridine derivatives to generate RTP and to mimic the photosynthesis for near-infrared cell imaging.

In this work, we successfully constructed a Q[8]-BCPI supramolecular assembly capable of emitting green phosphorescence at room temperature. This assembly was utilized for the detection of L-tryptophan and L-tyrosine, as well as for imaging HeLa cells. Notably, the crystal structure of the Q[8]-BCPI assembly was elucidated. The guest molecule BCPI consisted of the classical phosphorescent chromophore 6-bromoisoquinoline and the electron acceptor *p*-hydroxybenzonitrile (Scheme S1 in Supporting information), which were linked by a carbon chain to form a donor-acceptor (D-A) molecule. The successful preparation of BCPI was verified by the obtained single-crystalline structure and by ^{1}H and ^{13}C NMR spectra (Figs. S1–S5 and Table S1 in Supporting information).

As presented above, the Q[*n*]s possessed a rigid cavity. If the BCPI matches the size of this molecular cavity, it will be able to

* Corresponding author.
E-mail address: xxiao@gzu.edu.cn (X. Xiao).

https://doi.org/10.1016/j.cclet.2024.110022
1001-8417/

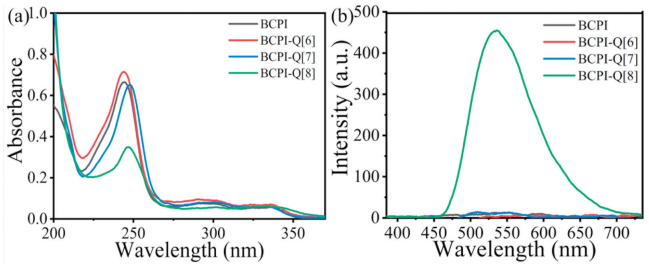

Fig. 1. (a) UV–vis spectra and (b) phosphorescence spectra of free BCPI, BCPI and Q[*n*] (*n* = 6–8). [BCPI] = 10 μmol/L, [Q[*n*]] = 30 μmol/L.

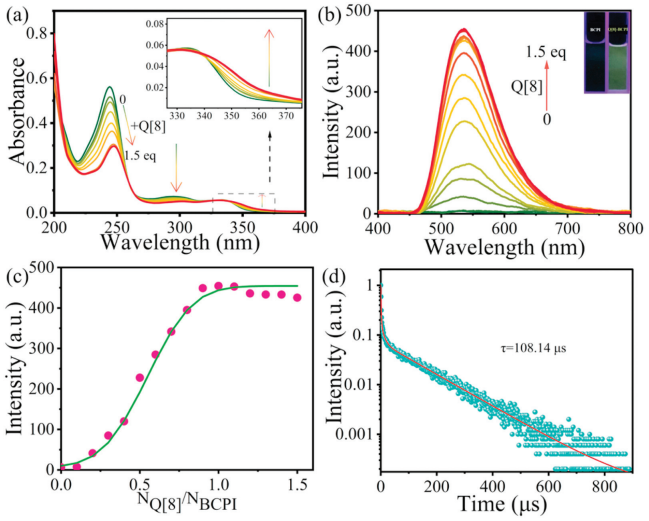

Fig. 2. (a) The UV–vis and (b) phosphorescent spectra of BCPI (10 μmol/L) in the presence of an increasing amount of Q[8] from 0, 0.1 … equiv. to 1.5 equiv., Inset: photographs of BCPI before and after (right) addition of 1.5 equiv. of Q[8] illuminated by the UV lamp at 254 nm. (c) The change of phosphorescent intensity at the wavelength of 534 nm. (d) Phosphorescent lifetime of 534 nm.

inhibit the vibration and rotation of the BCPI molecule, thereby producing phosphorescence emission [42]. Therefore, the Q[*n*]s have here been chosen as host molecules. As the first step, Q[*n*]s with a suitable cavity were selected as host molecules. Due to the D-A structure of the BCPI molecule and charge transfer (CT) [44,45], it was predicted that both ends of the alkyl chain of BCPI could be simultaneously positioned in the cavity of the Q[*n*]s. The Q[*n*]-BCPI host-guest complex was, thereby, formed, which contributed to the RTP emission [44,46]. These interactions were also analyzed by UV–vis spectra and phosphorescence spectra (Fig. 1 and Fig. S6 in Supporting information). When each of three Q[*n*]s (*n* = 6, 7, or 8) were added to the BCPI, the intensities of their resulting UV–vis spectra were different. However, phosphorescence emission was only produced for the addition of Q[8]. Interestingly, the aqueous solution emitted a visible green light under UV light irradiation at 254 nm [47].

Since the cavity size of Q[8] was matched with BCPI, the BCPI could enter the cavity of Q[8] to form supramolecular assembly and generate phosphorescence emission. Firstly, with a gradual addition of Q[8], the original UV absorption peaks were red-shifted and decreased in intensity (Fig. 2a). In addition, a new absorption peak appeared above 340 nm, which indicated that the spatial proximity of the functional groups at the end of the alkyl chain was the cause of the CT phenomenon. Due to the confinement effect of the macrocyclic hydrophobic cavity, the CT effect was generated, which promoted the generation of phosphorescence emission. This result implied that the ISC process was enabled by the host-enhanced CT effect.

Subsequently, the ITC analyses (Fig. S7 and Table S2 in Supporting information) showed that the enthalpy value (ΔH) that was associated with this incorporation was −34.94 kJ/mol, the entropy value ($T\Delta S$) was 5.34 kJ/mol, and the binding constant was 1.134×10^7 mol/L. Such a high binding constant indicated a relatively strong host-guest interaction between Q[8] and BCPI. Also, the binding of Q[8] to BCPI was most probably driven by the favorable enthalpy change, which was accompanied by a certain degree of entropic increase. Furthermore, the analyses by scanning electron microscopy (SEM) showed that the Q[8]-BCPI assembly had been successfully formed (Fig. S8 in Supporting information). By the use of the molar ratio method (Figs. 2b and c), Job's plot (Fig. S9 in Supporting information) and ITC experiments, they were also found that Q[8] and BCPI could form host-guest complexes with a host-to-guest molar ratio of 1:1 or n:n. The BCPI was then folded in the Q[8] cavity, where the benzene and naphthalene rings at the ends of the alkyl chain formed a π-π stacking. For the other situation (*i.e.*, n:n ratio), the BCPI molecules were wrapped head-to-tail in the Q[8] cavity, forming an n:n supramolecular assembly with a π-π stacking [48]. It showed a lifetime of 108.14 μs (Fig. 2d and Fig. S10 in Supporting information) and a quantum yield of 1.2% (Fig. S11 in Supporting information).

Analyses with ^{1}H NMR (Figs. S12 and S13 in Supporting information) were, thereafter, performed. As a result, the proton signals of the BCPI were all shifted to higher fields with the addition of Q[8]. It was only the degree of proton displacement that was different (Table S3 in Supporting information). These observations indicated that the whole BCPI molecule was located in the cavity of Q[8]. It was confirmed that the interaction ratio between BCPI and Q[8] was 1:1, and that the assembly was in a dynamic equilibrium in the aqueous solution. It was then assumed that the following assemblies of Q[8]-BCPI were formed in the aqueous solution: (1) The alkyl chain of the BCPI molecule had become partially folded, and the whole molecule had entered into the Q[8] cavity in this folded mode. (2) The isobromoquinoline portion of one of the BCPI molecules and the benzonitrile portion of the other BCPI molecule had formed a head-to-tail stacking in the cavity of Q[8], forming an n:n supramolecular assembly. There was also the possibility that the two BCPI molecules of isobromoquinoline formed an n:n supramolecular assembly by π-π stacking in the Q[8] cavity.

When culturing crystals, the introduction of metal ions can accelerate the production of Q[*n*] crystals by interactions with small molecules [49]. $ZnCl_2$ has here been used as an inducing reagent to obtain crystals of Q[8]-BCPI. The X-ray diffraction (XRD) analysis revealed a single-crystalline structure (Table S4 in Supporting information), with a *P*-1 space group. The asymmetric unit contained four Q[8] molecules, which have for convenience been numbered in Fig. 3a.

The presence of a large number of hydrogen bonds between different Q[8]s, and between Q[8] and the encapsulated BCPI guest, contributed to the formation of stable complexes (Figs. 3b–d). There was a C–H···π interaction between the bridged methylene group on the outer surface of Q[8] and the benzene ring of BCPI, in addition to a π-π stacking of isobromoquinolines of the same color. As well as differences in the direction and number of noncovalent interactions acting on BCPI led to three different types of stretching when BCPI interacted with Q[8] (Fig. S14 in Supporting information).

Moreover, the biocompatibility of Q[8]-BCPI was examined. After culturing with different concentrations of Q[8]-BCPI (0, 25, 50, 100, and 200 μmol/L) for 24 h, the surviving rate of the HeLa cells remained ≥80% (*n* = 4), which indicated a low cytotoxicity of Q[8]-BCPI for the living cells. Furthermore, after a co-culturing of the cells with 200 μmol/L Q[8]-BCPI for 8 h, the Q[8]-BCPI was found to be absorbed onto the living HeLa cells in the cytoplasm under the red channel (Fig. 4). Consequently, the cytocompatibility

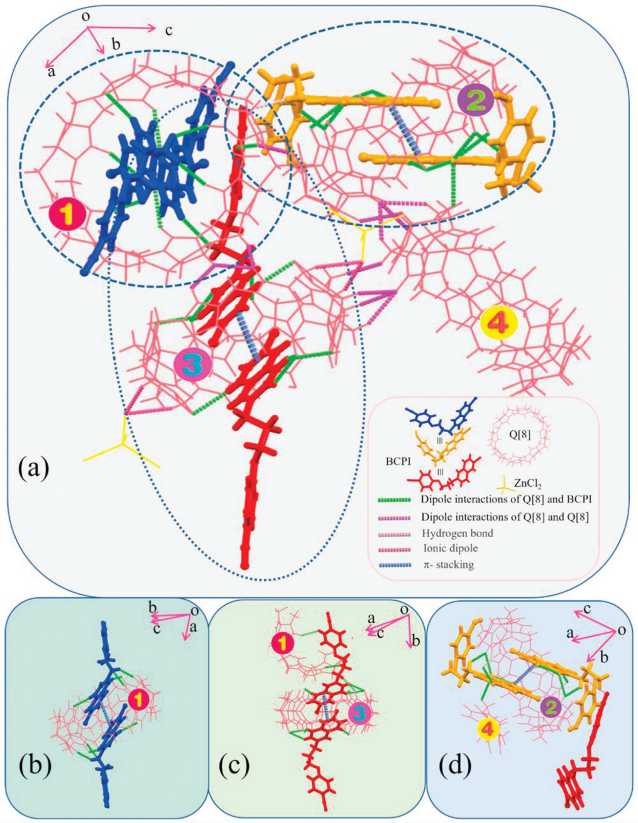

Fig. 3. (a) All the non-covalent interaction of the basic unit of Q[8]-BCPI. (b–d) Interactions between different Q[8] and BCPI.

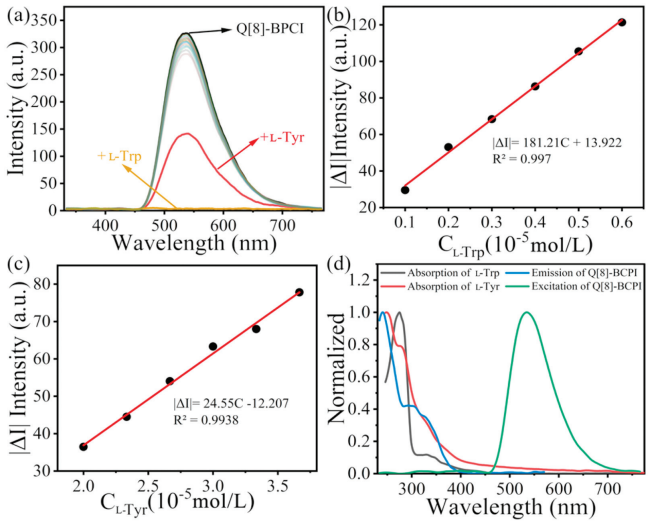

Fig. 5. (a) Phosphorescent spectra of Q[8]-BCPI in the presence of 10 equiv. of different essential amino acids. LOD plot of Q[8]-BCPI (10 μmol/L) toward (b) L-Trp and (c) L-Tyr. (d) Normalized spectra of the UV-vis absorption spectra of L-Trp and L-Tyr, phosphorescence excitation/emission spectra of Q[8]-BCPI (The green line represents the excitation of Q[8]-BCPI, the blue line corresponds to the emission of Q[8]-BCPI, the red line indicates L-Tyr, and the black line represents L-Trp).

and tracing capability of Q[8]-BCPI within living cells could be confirmed, enabling visualization of the transport processes between the cells by this assembled supramolecule. Thus, this confirmation serves as a prerequisite for the potential applications of Q[8]-BCPI in organisms.

Moreover, Q[8] and BCPI formed the supramolecular assembly Q[8]-BCPI, which produced excellent green RTP in aqueous solution that could be used for analytical detection. More specifically, it could be used to recognise L-Tyr and L-Trp (Fig. 5a and Fig. S15 in Supporting information), which greatly improved the accuracy of the used assay. The incorporation of L-Trp led to a phosphorescence quenching of the assemblies. The limit of detection (LOD) was calculated as 6.353×10^{-7} mol/L by a highly correlated linear function (Fig. 4b, Figs. S16 and S17 in Supporting information). Also, the addition of L-Tyr led to a diminished phosphorescence intensity, with a highly correlated linear function and a calculated LOD value of 4.689×10^{-6} mol/L (Fig. 4c, Figs. S19 and S20 in Supporting information). The responses of Q[8]-BCPI to various interfering substances had also been analyzed (Figs. S18 and S21 in Supporting information). It was then shown that Q[8]-BCPI was selective for L-Tyr and L-Trp, and not susceptible to interferences by other essential amino acids. Furthermore, we conducted a comparative analysis of the detection capabilities of Q[*n*] probes for amino acids, revealing that Q[8]-BCPI exhibited superior detection performance as shown in Table S5 (Supporting information).

As the next step, the mechanism by which the Q[8]-BCPI phosphorescence changed upon addition of L-Trp, or L-Tyr, was explored. As a result of the ^{1}H NMR analyses, both L-Trp and L-Tyr had no effect on either Q[8]-BCPI or BCPI. Thus, a competition-induced phosphorescence quenching could be ruled out (Figs. S22–S25 in Supporting information). To investigate the potential for electrostatic interaction, we examined the zeta potential upon the addition of L-Trp and L-Tyr to Q[8]-BCPI individually. As depicted in Fig. S26 (Supporting information), the zeta potential of Q[8]-BCPI@L-Trp was −4.26 mV, lower than that of Q[8]-BCPI (2.32 mV). Similarly, the zeta potential of Q[8]-BCPI@L-Tyr was −11.47 mV, also lower than that of Q[8]-BCPI (2.32 mV). These findings suggest that the positively charged Q[8]-BCPI supramolecular assembly engages in electrostatic interactions with L-Trp and L-Tyr, respectively [50]. Moreover, the absorption spectra of L-Trp and

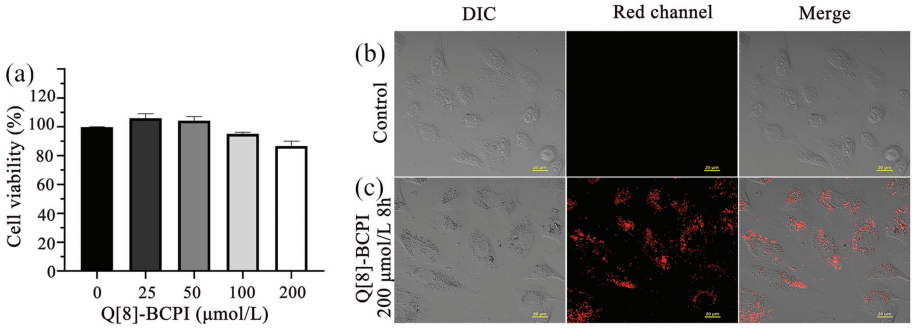

Fig. 4. (a) Cell viability after 24 h incubation of different concentrations of Q[8]-BCPI in HeLa cells; confocal laser scanning micrographs of HeLa cells co-stained with free (b); 200 μmol/L Q[8]-BCPI for 8 h (c). Scale bar: 20 μm.

L-Tyr exhibited significant overlap with the excitation spectrum of Q[8]-BCPI (Fig. 5d). Upon the addition of L-Trp or L-Tyr to Q[8]-BCPI, a decrease in the peak at 534 nm was observed in the phosphorescence spectra (Fig. S26). These results imply that the Q[8]-BCPI supramolecular assembly may exhibit an internal filtration effect (IFE) with L-Trp and L-Tyr, respectively [51–53]. Collectively, these results suggest that the combined impact of electrostatic interaction and IFE is likely the primary mechanism underlying this quenching.

In the present study, a supramolecular assembly has been constructed by using Q[8] and BCPI molecules. The hydrophobic cavity and size of Q[8] suppressed the rotational vibrations of the BCPI molecules. The ICT effect was, thereby, also enhanced, which caused the excellent green RTP properties of Q[8]-BCPI. The crystal structure also further confirms that the Q[8] cavity is encapsulated with 6-bromoisoquinoline phosphorescent groups thus producing RTP. The Q[8]-BCPI assembly has, therefore, the capability to recognize the essential amino acids L-Trp and L-Tyr, with L-Trp leading to a green phosphorescence quenching and L-Tyr leading to a decreased green phosphorescence intensity (synergistic effect of electrostatic interaction and IFE). Moreover, Q[8]-BCPI showed excellent biocompatibility and minimal biotoxicity. In addition, it demonstrated a strong staining effect on the HeLa cells. The present study has broadened the use of Q[n] for bioimaging, and uncovered their potential for use in innovative phosphorescent materials.

Declaration of competing interest

The authors declare that they have no known competing financial interests or personal relationships that could have appeared to influence the work reported in this paper.

Acknowledgments

This work was supported by the National Natural Science Foundation of China (No. 22361011) and Guizhou Provincial Science and Technology Projects (No. ZK [2023] General 040).

Supplementary materials

Supplementary material associated with this article can be found, in the online version, at doi:10.1016/j.cclet.2024.110022.

References

[1] Y.Y. Si, Y.Y. Zhao, W.B. Dai, et al., Chin. J. Chem. 41 (2023) 1575–1582.
[2] H. Gao, Z. Gao, D. Jiao, et al., Small 17 (2021) 2005449.
[3] W.L. Zhou, W. Lin, Y. Chen, et al., Chem. Sci. 13 (2022) 7976–7989.
[4] B.B. Ding, X. Ma, H. Tian, Acc. Mater. Res. 4 (2023) 827–838.
[5] F. Gu, X. Ma, Chem. Eur. J. 28 (2022) e202104131.
[6] H. Ju, H. Zhang, L.X. Hou, et al., J. Am. Chem. Soc. 145 (2023) 3763–3773.
[7] Y. Zhu, Z. Feng, Z. Yan, et al., Sens. Actuator. B: Chem. 371 (2022) 132529.
[8] S. Kuila, K.V. Rao, S. Garain, et al., Angew. Chem. Int. Ed. 57 (2018) 17115–17119.
[9] X.K. Ma, Q.W. Cheng, X.L. Zhou, et al., JACS Au 3 (2023) 2036–2043.
[10] D. Li, Z. Liu, M. Fang, et al., ACS Nano 17 (2023) 12895–12902.
[11] H.J. Wang, W.W. Xing, Z.H. Yu, et al., Adv. Opt. Mater. 10 (2022) 2201903.
[12] W. Zhu, H. Xing, E. Li, et al., Macromolecules 55 (2022) 9802–9809.
[13] P. Wei, X. Zhang, J. Liu, et al., Angew. Chem. Int. Ed. 59 (2020) 9293–9298.
[14] H. Zhu, J. Liu, Y. Wu, et al., J. Am. Chem. Soc. 145 (2023) 11130–11139.
[15] J. Wang, Z. Huang, X. Ma, et al., Angew. Chem. Int. Ed. 59 (2020) 9928–9933.
[16] C. Li, Q. Guo, J. Zhu, et al., Res. Chem. Intermed. 49 (2023) 2755–2768.
[17] C. Li, X. Li, Q. Wang, Chin. Chem. Lett. 33 (2022) 877–880.
[18] D. Yang, M. Liu, X. Xiao, et al., Coord. Chem. Rev. 434 (2021) 213733.
[19] W. Zhang, Y. Luo, J. Zhao, et al., Chin. Chem. Lett. 33 (2021) 2455–2458.
[20] R. Cen, M. Liu, H. Xiao, et al., Sens. Actuator. B: Chem. 378 (2022) 133126.
[21] Y. Luo, W. Zhang, M. Liu, et al., Chin. Chem. Lett. 32 (2020) 367–370.
[22] J.H. Hu, Y. Huang, R. Carl, et al., Coord. Chem. Rev. 489 (2023) 215194.
[23] R.H. Gao, L.X. Chen, K. Chen, et al., Coord. Chem. Rev. 348 (2017) 1–24.
[24] W. Zhang, Y. Luo, Y. Zhou, et al., Dyes Pigments 176 (2020) 108235.
[25] M. Liu, R. Cen, J. Li, et al., Angew. Chem. Int. Ed. 61 (2022) e202207209.
[26] M. Liu, R. Cen, J.H. Lu, et al., Chin. Chem. Lett. 33 (2021) 2469–2472.
[27] Y. Luo, W. Zhang, J. Zhao, et al., Chin. Chem. Lett. 34 (2022) 107780.
[28] A. Hennig, H. Bakirci, W.M. Nau, Nat. Methods 4 (2007) 629–632.
[29] H. Barbero, N.A. Thompson, E. Masson, J. Am. Chem. Soc. 142 (2020) 867–873.
[30] X. Yang, Q. Cheng, V. Monnier, et al., Angew. Chem. Int. Ed. 60 (2021) 6617–6623.
[31] X. Yang, F. Liu, Z. Zhao, et al., Chin. Chem. Lett. 29 (2018) 1560–1566.
[32] L. Xu, L. Zou, H. Chen, et al., Dyes Pigments 142 (2017) 300–305.
[33] B.S. Kanti, P.S. Kumar, B. Supratim, Chem. Commun. 59 (2023) 10396–10399.
[34] W. Zhang, Y. Luo, C. Liu, et al., ACS Appl. Mater. Interfaces 14 (2022) 51429–51437.
[35] C. Li, J. Zhu, Q. Wang, Dyes Pigments 204 (2022) 110368.
[36] M. Singh, K. Liu, S. Qu, et al., Adv. Opt. Mater. 9 (2021) 2002197.
[37] X.K. Ma, Y. Liu, Acc. Chem. Res. 17 (2021) 3403–3414.
[38] S.K. Bhaumik, R. Biswas, S. Banerjee, Chem. Asian J. 16 (2021) 2195–2210.
[39] D.A. Xu, Q.Y. Zhou, X. Dai, et al., Chin. Chem. Lett. 33 (2022) 851–854.
[40] X. Yu, W. Liang, Q. Huang, et al., Chem. Commun. 55 (2019) 3156–3159.
[41] H.J. Yu, Q. Zhou, X. Dai, et al., J. Am. Chem. Soc. 34 (2021) 13887–13894.
[42] W.W. Xing, H.J. Wang, Z. Liu, et al., Adv. Opt. Mater. 11 (2023) 2202588.
[43] Y.H. Liu, Y. Liu, J. Mater. Chem. B 10 (2022) 8058–8063.
[44] J. Yang, X. Hu, M. Fan, et al., Org. Chem. Front. 10 (2023) 422–429.
[45] C. Liu, X. Xiao, X.L. Ni, Dyes Pigments 212 (2023) 111152.
[46] H.J. Yu, Q. Zhou, X. Dai, et al., J. Am. Chem. Soc. 143 (2021) 13887–13894.
[47] H.G. Nie, Z. Wei, X.L. Ni, et al., Chem. Rev. 122 (2022) 9032–9077.
[48] X.K. Ma, W. Zhang, Z. Liu, et al., Adv. Mater. 33 (2021) 2007476.
[49] X.L. Ni, X. Xiao, H. Cong, et al., Chem. Soc. Rev. 42 (2013) 9480–9508.
[50] A. Bahadoran, M.K. Jabarabadi, Z.H. Mahmood, et al., Spectrochim. Acta Part A: Mol. Biomol. Spectrosc. 268 (2022) 118863.
[51] J. Xiong, S. He, Z. Wang, et al., J. Hazard. Mater. 429 (2022) 128316.
[52] J. Zhang, X. Lu, Y. Lei, et al., Nanoscale 9 (2017) 15606–15611.
[53] S. Ghosh, J. Krishnan, S.S. Hossain, et al., ACS Appl. Mater. Interfaces 15 (2023) 26843–26851.